Electronic Supplementary Material (ESI) for RSC Advances.
This journal is © The Royal Society of Chemistry 2022

NS3 helicase inhibitory potential of the marine sponge *Spongia irregularis*

Enas Reda Abdelaleem[a,Φ], Mamdouh Nabil Samy[a,Φ], Taha F. S. Ali[b], Muhamad Mustafa[c], Mahmoud A. A. Ibrahim[d] , Gerhard Bringmann[e], Safwat A. Ahmed[f], Usama Ramadan Abdelmohsen[a,g,*], Samar Yehia Desoukey[a]

[a]Department of Pharmacognosy, Faculty of Pharmacy, Minia University, 61519Minia, Egypt.

[b]Department of Medicinal Chemistry, Faculty of Pharmacy, Minia University, 61519 Minia, Egypt.

[c]Medicinal Chemistry Department, Faculty of Pharmacy, Deraya University, New Minia 61111, Egypt.

[d]Computational Chemistry Laboratory, Chemistry Department, Faculty of Science, Minia University, 61519Minia, Egypt.

[e]Institute of Organic Chemistry, University of Würzburg, Am Hubland, 97074 Würzburg, Germany.

[f]Department of Pharmacognosy, Faculty of Pharmacy, Suez Canal University, Ismailia 41522, Egypt.

[g]Department of Pharmacognosy, Faculty of Pharmacy, Deraya University, New Minia 61111, Egypt.

* Corresponding author, [Φ] Equal contribution.

Table S1: List of secondary metabolites annotated from the ethyl acetate fraction *of Spongia irregularis*.

N.	Compound	Accurate mass	Mode	*m/z*	R_t	Structure	Source	Reference
5	19,20 Dihydroxyspongia-13(16),14-diene	318.2195	+	319.2233	3.40	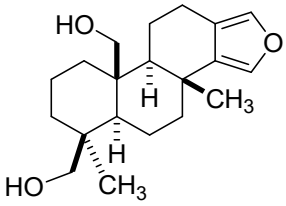	*Spongia* Sp.	[1]
6	3*β*-Acetoxyspongia-13(16),14-diene	344.2351	-	343.2258	2.32	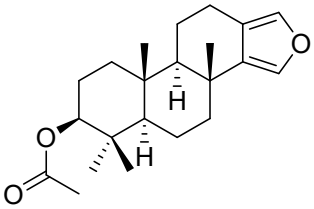	*Spongia* Sp.	[2]
7	3*α*-Acetoxyspongia-13(16),14-diene					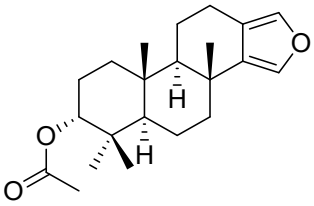	*Spongia* Sp.	
8	Ceylonamide H	345.2304	+	346.2391	2.33	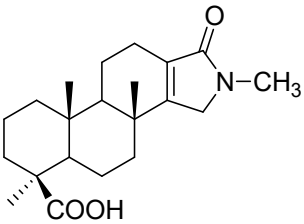	*Spongia* Sp.	[3]
9	5-Epi-isospongiaquinone	358.2114	-	357.2039	2.86	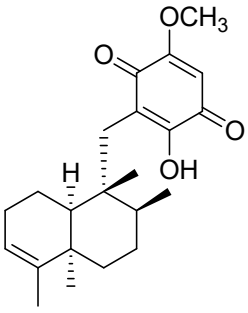	*Spongia hispida*	[4]

10	Spongiacysteine	363.2079	_	362.2035	2.95	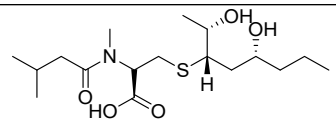	*Spongia* Sp.	[5]
11	Rhopaloic acid c	372.2664	+	373.2638	3.03	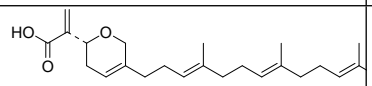	*Hippospongia* sp.	[6]
12	1,4,44-Trihydroxy-2-octaprenylbenzene	670.5325	-	669.5264	3.28	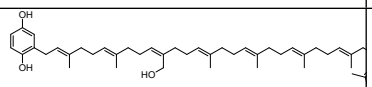	*Spongia* Sp.	[7]
13	Nakijiquinone E	713.4291	-	712.4287	3.27	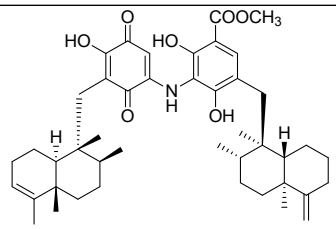	*Spongia* Sp.	[8]
14	Nakijiquinone F					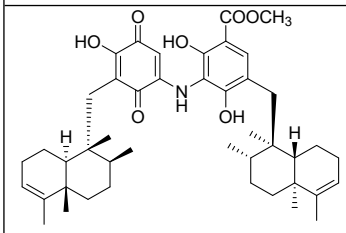	*Spongia* Sp.	

Table S2: Docking results of the top-ranked docking pose (Compound **13**) with the active site of HCV NS3 protease compared to the co-crystallized ligand.

Ligand	**Binding affinity (ΔG in Kcal/mol)**	**Interaction parameters**			
		Interaction	AA Residue	δ(Å)	E (Kcal/mol)
Co-crystallized ligand	-11.3	H-donor	Arg 1155	2.82	-4.6
		H-donor	His 1057	3.01	-7.5
		H-donor	Ala 1157	2.88	-4.3
		H-acceptor	Gly 1137	3.00	-1.1
		H-acceptor	Gly 1137	3.02	-2.8
		H-acceptor	Ala 1157	2.95	-3.7
		H- π	His 1057	3.68	-1.6
13	-7.0				

Table S3: Docking results of the top-ranked docking pose (Compound **13**) with HCV NS5B polymerase's active site compared to the co-crystallized ligand.

Ligand	**Binding affinity (ΔG in Kcal/mol)**	**Interaction parameters**			
		Interaction	AA Residue	δ(Å)	E (Kcal/mol)
Co-crystallized ligand	-9.6	H-donor	Asp 318	2.71	-7.2
		H-acceptor	Ser 556	3.11	-1.0
		H-acceptor	Asn 291	2.88	-3.5
		H- π	Met 414	4.77	-0.5
13	-9.5	H-donor	Cys 366	2.61	-2.9
		H-acceptor	Ser 367	2.85	-1.9

Table S4: Docking results of the top-ranked docking pose (Compound **14**) with the active site of HCV Helicase compared to the co-crystallized ligand.

Ligand	**Binding affinity (ΔG in Kcal/mol)**	**Interaction parameters**			
		Interaction	AA Residue	δ(Å)	E (Kcal/mol)
Co-crystallized ligand	-7.5	H-donor	Trp 501	2.81	-2.3
		H-acceptor	Gly 255	2.91	-3.5
		H-acceptor	Gly 255	2.92	-4.6
		H-acceptor	Thr 269	3.52	-1.9
14	-7.4	H-donor	Asn 556	3.30	-0.2
		H- acceptor	Trp 501	2.96	-1.7
		H- π	Trp 501	3.84	-0.4
		H- π	Trp 501	4.04	-0.4
		H- π	Trp 501	4.17	-0.9

Table S5: Docking results of the top-ranked docking pose (Compound **14**) with the active site of HCV Protease-Helicase allosteric site compared to the co-crystallized ligand.

Ligand	**Binding affinity (ΔG in Kcal/mol)**	**Interaction parameters**			
		Interaction	AA Residue	δ(Å)	E (Kcal/mol)
Co-crystallized ligand	-9.0	H-donor	Asp 79	3.46	-0.7
		H-donor	Cys 525	3.00	-4.2
		H-donor	H_2O (Glu	3.04	-5.3
		H-donor	628)	2.99	-1.1
		H-acceptor	Leu 517	2.97	-4.8
			Cys 525		
14	-10.1	H-donor	Asp 79	3.58	-0.3
		H-donor	Glu 628	3.70	-0.8
		π - H	Val 524	4.47	-0.3

Table S6: Lipinski rule and drug-likeness of isolated and dereplicated compounds **1-14**.

Molecule	Number of violotions (Lipinski rule)	Mwt (g/mol)	H-bond donors	H-bond aaceptors	Number of rotatable Bonds	LogP
1	0	193.21	1	3	0	0.06
2	0	116.07	2	4	0	-0.49
3	0	242.23	3	5	2	-0.61
4	0	118.14	1	1	0	1.60
5	0	318.45	2	3	2	3.53
6	0	344.49	0	3	2	4.75
7	0	344.49	0	3	2	4.69
8	0	345.48	1	3	1	3.23
9	0	358.47	1	4	3	3.84
10	0	363.51	3	5	13	2.03
11	0	372.54	1	3	11	2.03
12	1, Mwt>500	671.05	3	3	24	2.03
13	2, Mwt>500, LogP>5	713.94	4	7	8	7.90
14	2, Mwt>500, LogP>5	713.94	4	7	8	7.81

Table S7: Medicinal chemistry properties of isolated and dereplicated compounds as well as their ADME parameters.

Molecule	GI absorption	Bioavilability score	Pgp substrate	BBB permeation	Synthetic accessibility
1	High	0.55	No	No	2.34
2	High	0.55	No	No	2.79
3	High	0.55	No	No	3.64
4	High	0.55	No	Yes	1.17
5	High	0.55	Yes	Yes	4.91
6	High	0.55	No	Yes	4.92
7	High	0.55	No	Yes	4.92
8	High	0.85	Yes	Yes	4.66
9	High	0.85	No	Yes	5.10
10	High	0.55	Yes	No	4.60
11	High	0.56	Yes	No	4.60
12	High	0.56	Yes	No	4.60
13	Low	0.56	Yes	No	7.56
14	Low	0.56	Yes	No	7.56

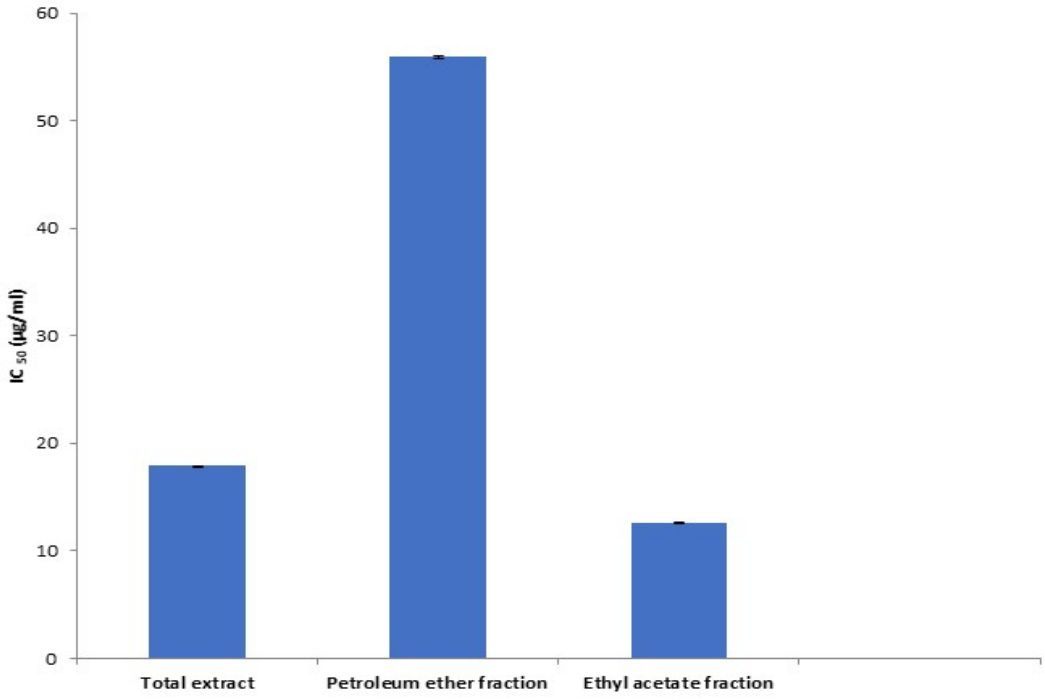

Figure S1: IC_{50} values of the anti-HCV activities of the total extract and two fractions of *S. irregularis.*

NMR spectroscopic analysis of compound (1-4):

1,3,7-Trimethylguanine (1):

^{1}H NMR (400 MHz, $CDCl_3$): δ= 7.54 (1H, s, H-8), 3.94 (3H, s, N_7- CH_3), 3.57 (3H, s, N_3-CH_3), 3.39 (3H, s, N_1- CH_3).
^{13}C NMR (100 MHz, $CDCl_3$): δ= 155.9 (C-6), 152.2 (C-2), 148.9 (C-4), 141.7 (C-8), 108.1 (C-5), 34.3 (N_7- CH_3), 30.5 (N_3- CH_3), 28.5 (N_1- CH_3).

3,5-Dihydroxyfuran-2(5H)-one (2):

^{1}H NMR (400 MHz, DMSO-*d6*): δ= 10.96 (2H, br s, OH groups), 7.38 (1H, d, *J*=7.6 Hz, H-4), 5.44 (1H, d, *J*=7.6 Hz, H-5)
APT^{13}C NMR (100 MHz, DMSO-*d6*): δ= 165.0 (C-2), 152.2 (C-3), 142.9 (C-4), 100.9 (C-5).

Thymidine (3):

^{1}H NMR (500 MHz, DMSO-*d6*): δ= 11.27 (NH, br s), 7.69 (1H, d, *J*= 1.2 Hz, H-4), 6.15 (1H, t, *J*= 6.3 Hz,H-1'), 5.26 (1H,br s, 3' OH), 5.05 (1H,br s, 5' OH), 4.23 (1H, br s, H-3'), 3.75 (1H, m, H-4'), 3.53 (2H, m, H-5'), 2.02-2.08 (2H, m, H-2'), 1.77 (3H, d, *J*= 1.2 Hz, 5-CH_3).
^{13}C NMR (125 MHz, DMSO-*d6*): δ= 164.3 (C-6), 150.9 (C-2), 136.6 (C-4), 109.8 (C-5), 87.3 (C-4'), 84.2 (C-1'), 70.9 (C-3'), 61.8 (C-5'), (C-2', Obscured by solvent), 12.7 (5-CH_3)**.**

1H-indazole (4):

^{1}H NMR (400 MHz, CD_3OD): δ= 8.07 (1H, dd, *J*= 1.6, 6.3,H-4), 7.94 (1H,s, H-3), 7.43 (1H, dd, *J*= 1.5, 6.6, H-7), 7.18 (1H, td, *J*= 1.4, 7.1, H-5), 7.15 (1H, td, *J*= 1.4, 7.1, H6), 4.6 (NH)
^{13}C NMR (100 MHz, CD_3OD): δ= 138.9 (C-7a), 133.9 (C-3), 128.4 (C-3a), 124.3 (C-6), 123.0 (C-4), 122.8 (C-5), 113.6 (C-7).

NMR spectroscopic analysis of compound (1):

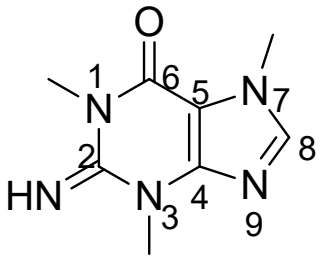

1,3,7-Trimethylguanine

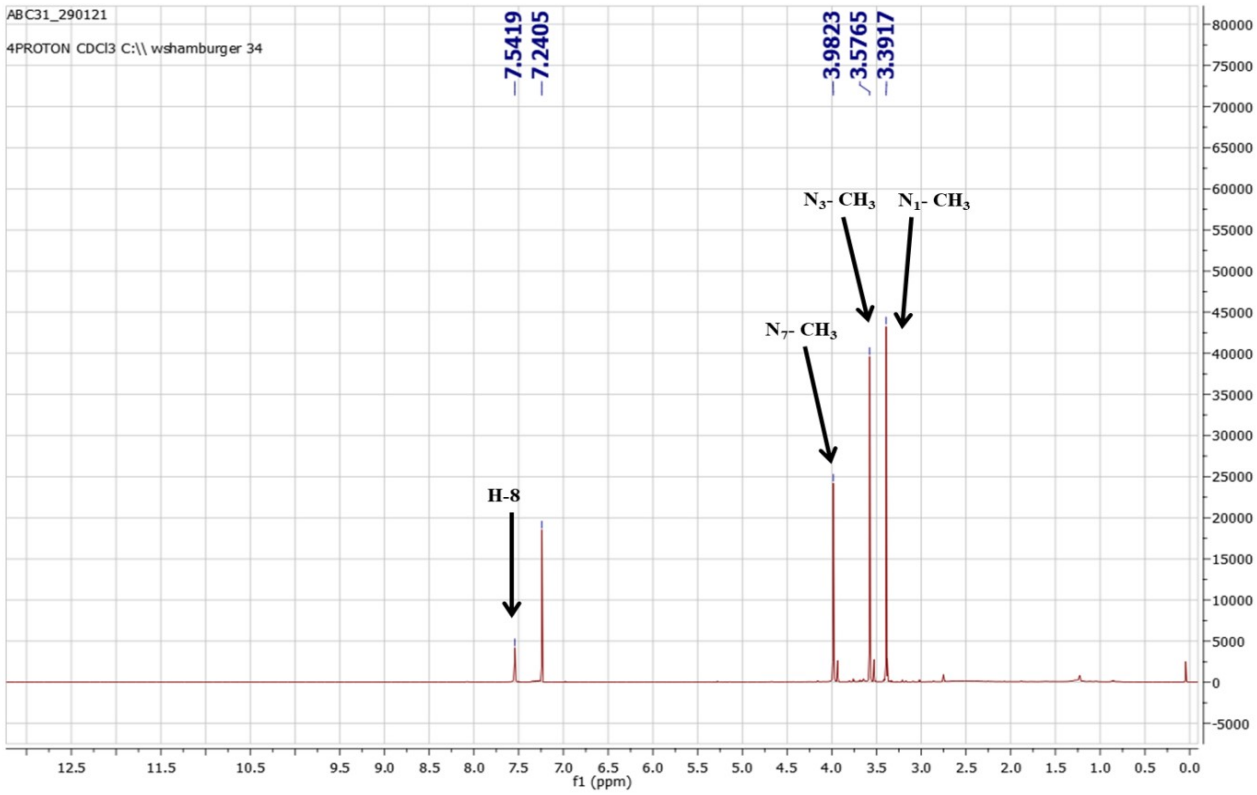

Figure S2: ^{1}H- NMR spectrum of compound **1** ($CDCl_3$, 400 MHz)

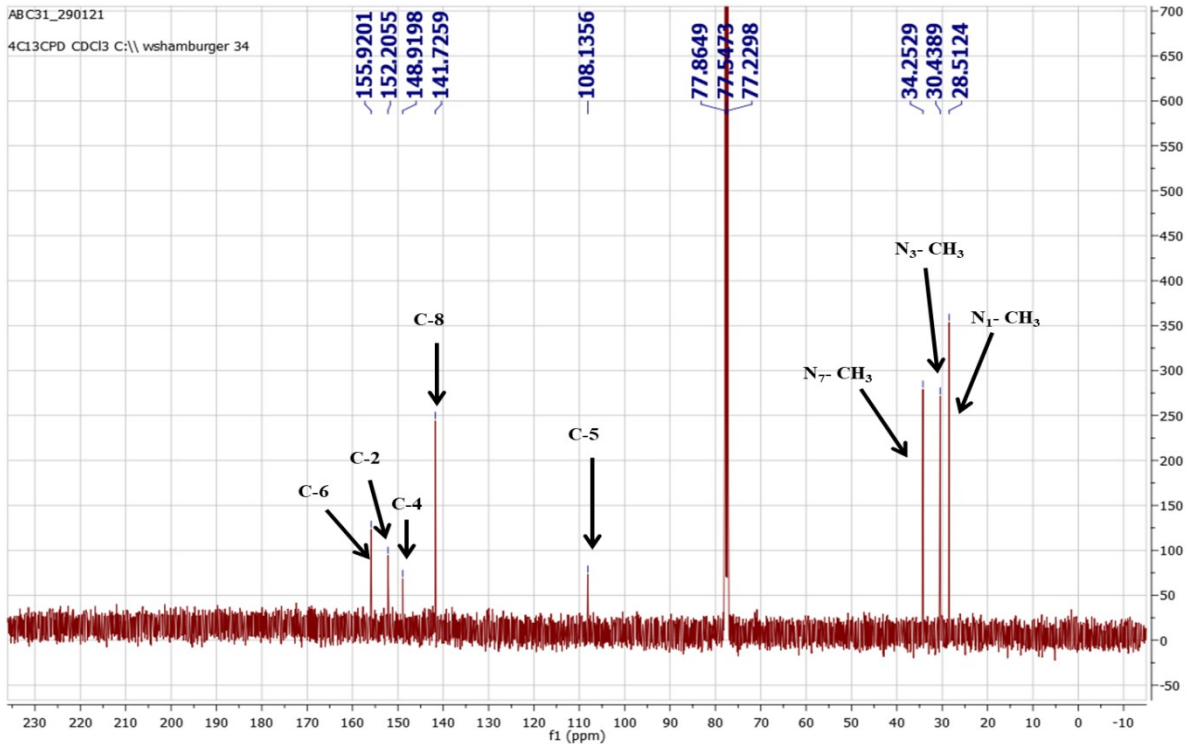

Figure S3: ^{13}C- NMR spectrum of compound **1** ($CDCl_3$, 100 MHz)

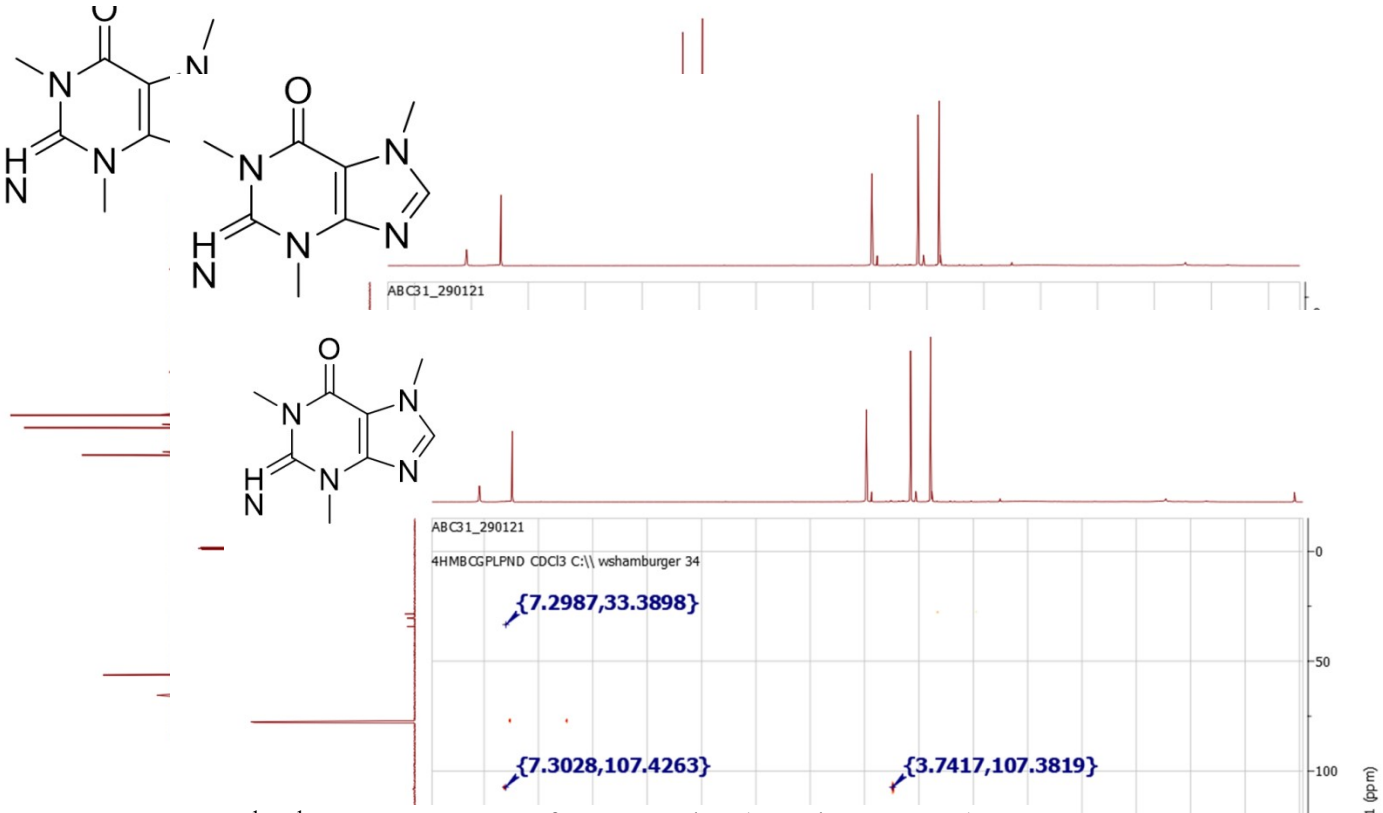

Figure S4: H^1-H^1 COSY spectrum of compound **1** ($CDCl_3$, 400 MHz)

Figure S5: HSQC spectrum of compound **1** ($CDCl_3$, 400 MHz)

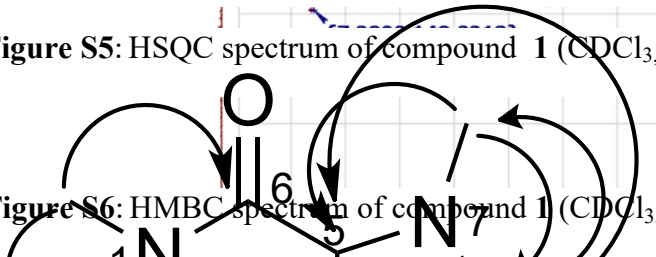

Figure S6: HMBC spectrum of compound **1** ($CDCl_3$, 400 MHz)

Figure S7: Significant HMBC correlations of compound **1**

NMR spectroscopic analysis of compound (2):

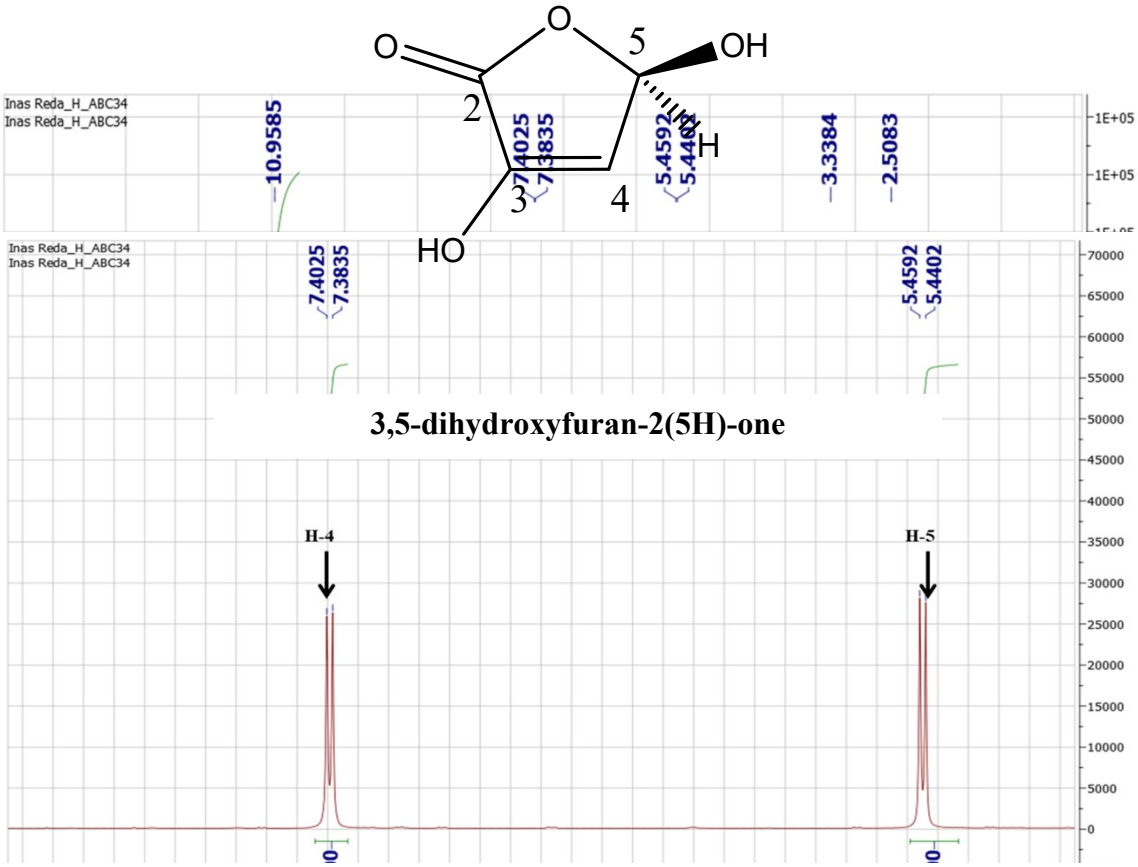

Figure S9: Expanded ^{1}H- NMR spectrum of compound **2** (DMSO-d_6, 400 MHz)

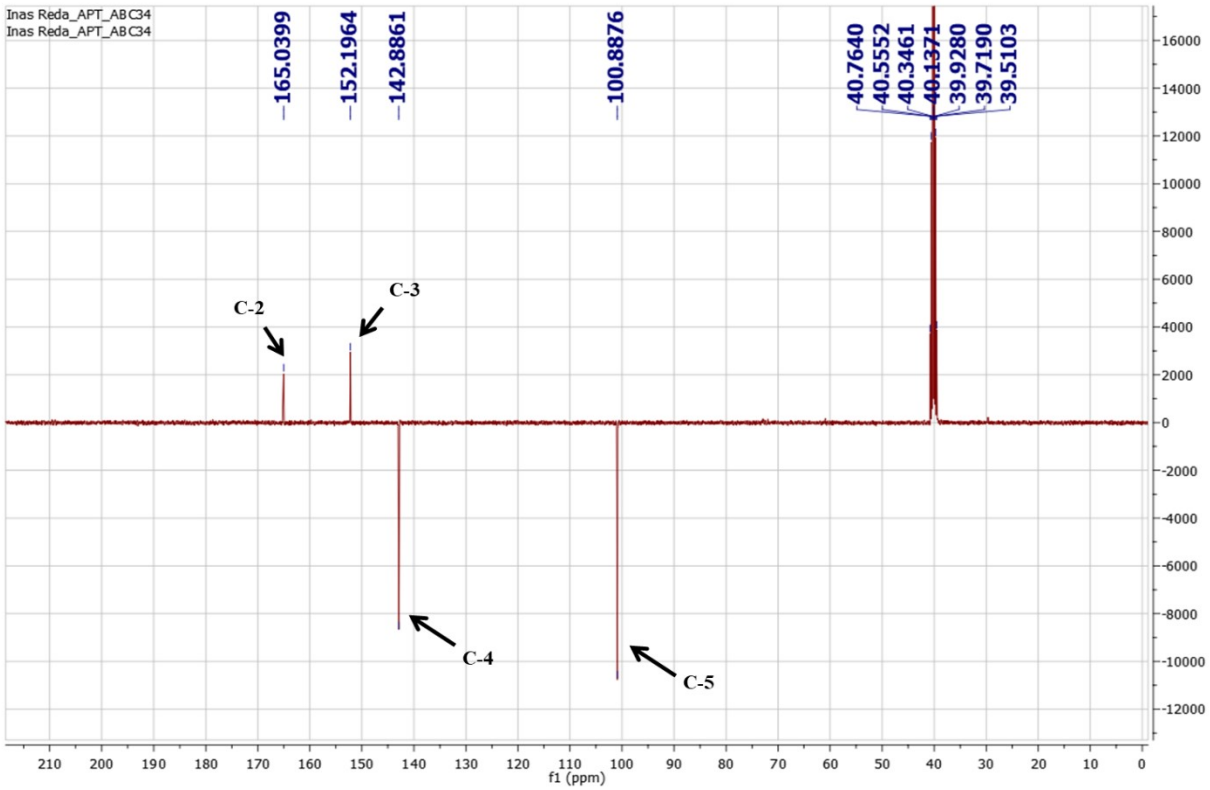

Figure S10: APT ^{13}C- NMR spectrum of compound **2** (DMSO-d_6, 100 MHz)

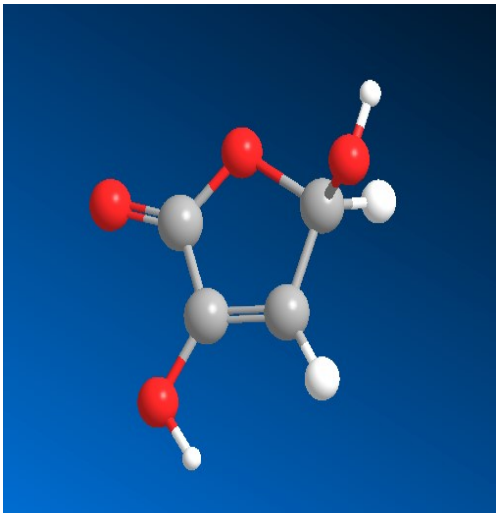

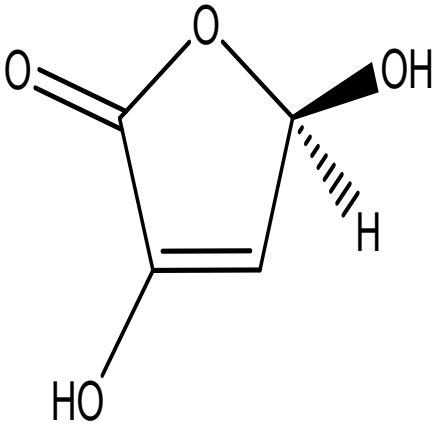

Figure S11: 3D structure of α-oriented proton of compound **2**

NMR spectroscopic analysis of compound (3):

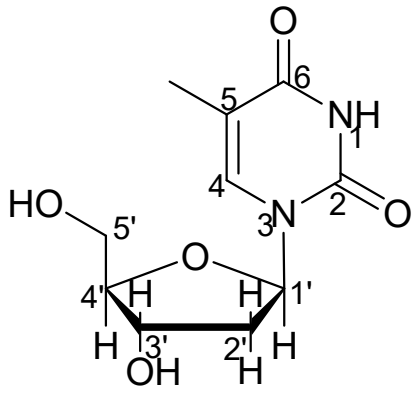

Thymidine

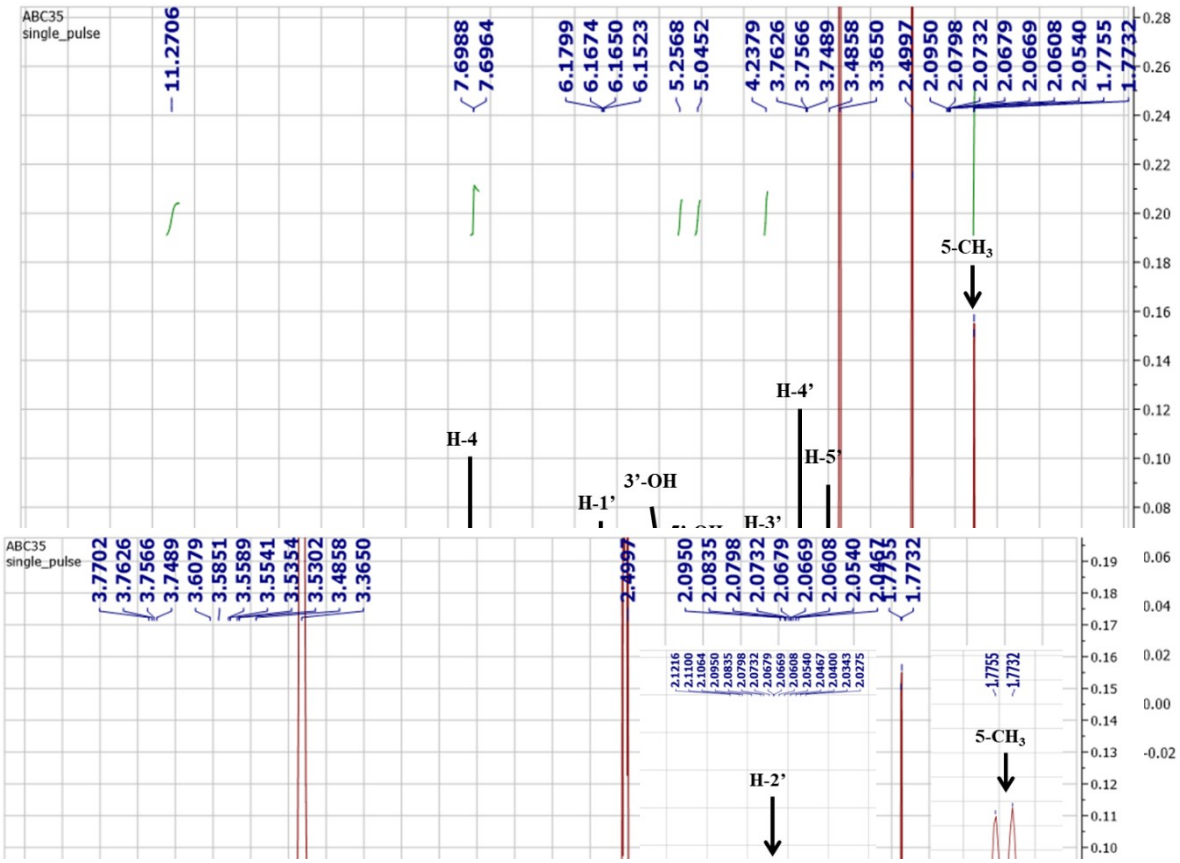

Figure S12: ^{1}H- NMR spectrum of compound **3** (DMSO-d_6, 500 MHz)

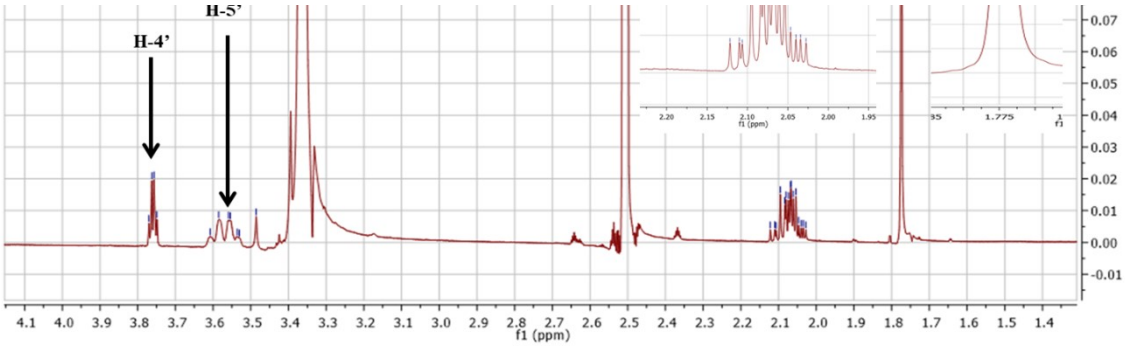

Figure S13: Expanded ^{1}H- NMR spectrum of compound **3** (DMSO-d_6, 500 MHz)

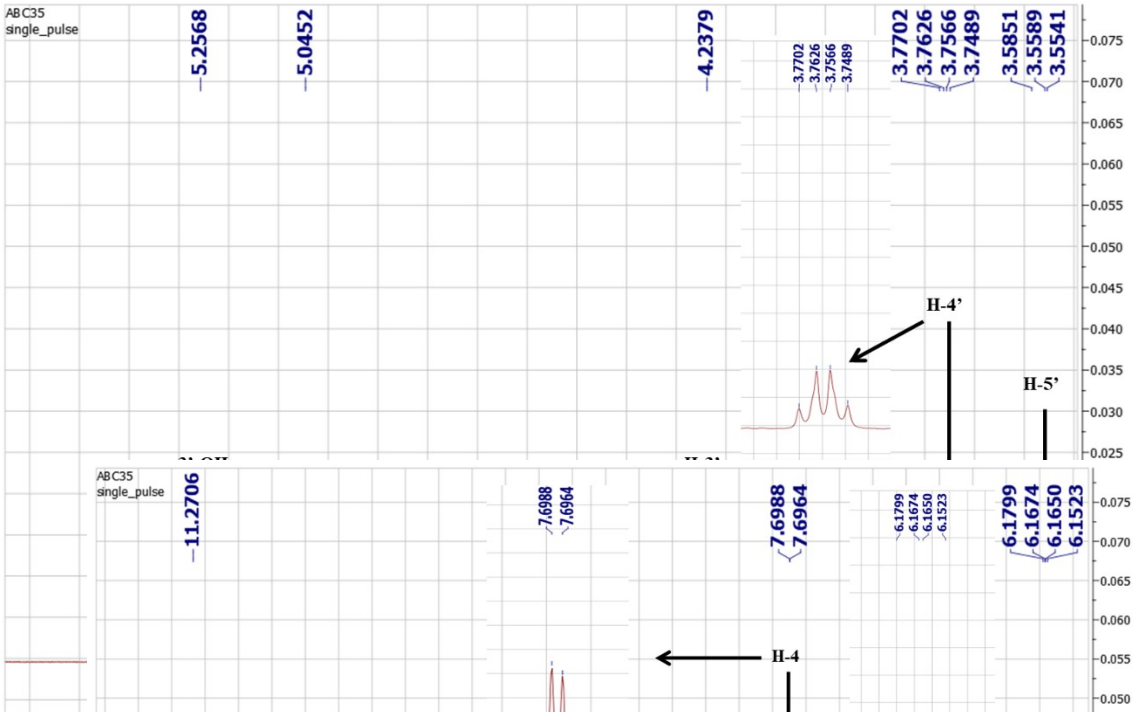

Figure S14: Expanded ^{1}H- NMR spectrum of compound **3** (DMSO-d_6, 500 MHz)

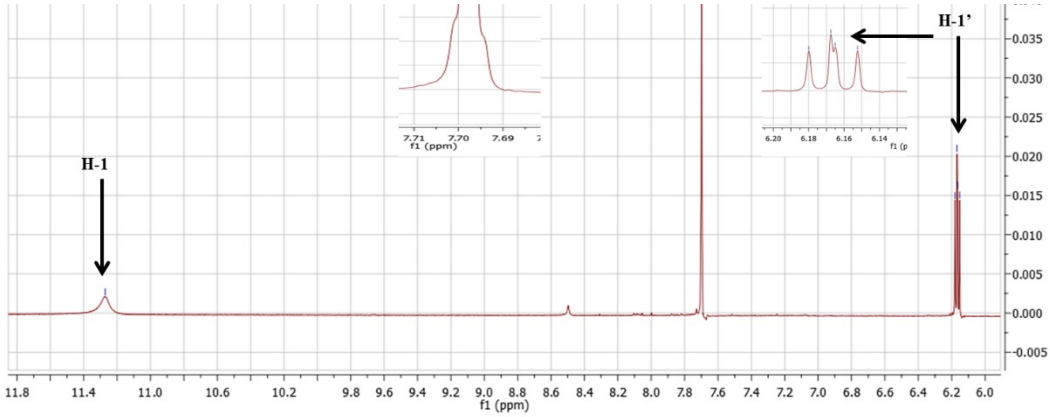

Figure S15: Expanded ^{1}H- NMR spectrum of compound **3** (DMSO-d_6, 500 MHz)

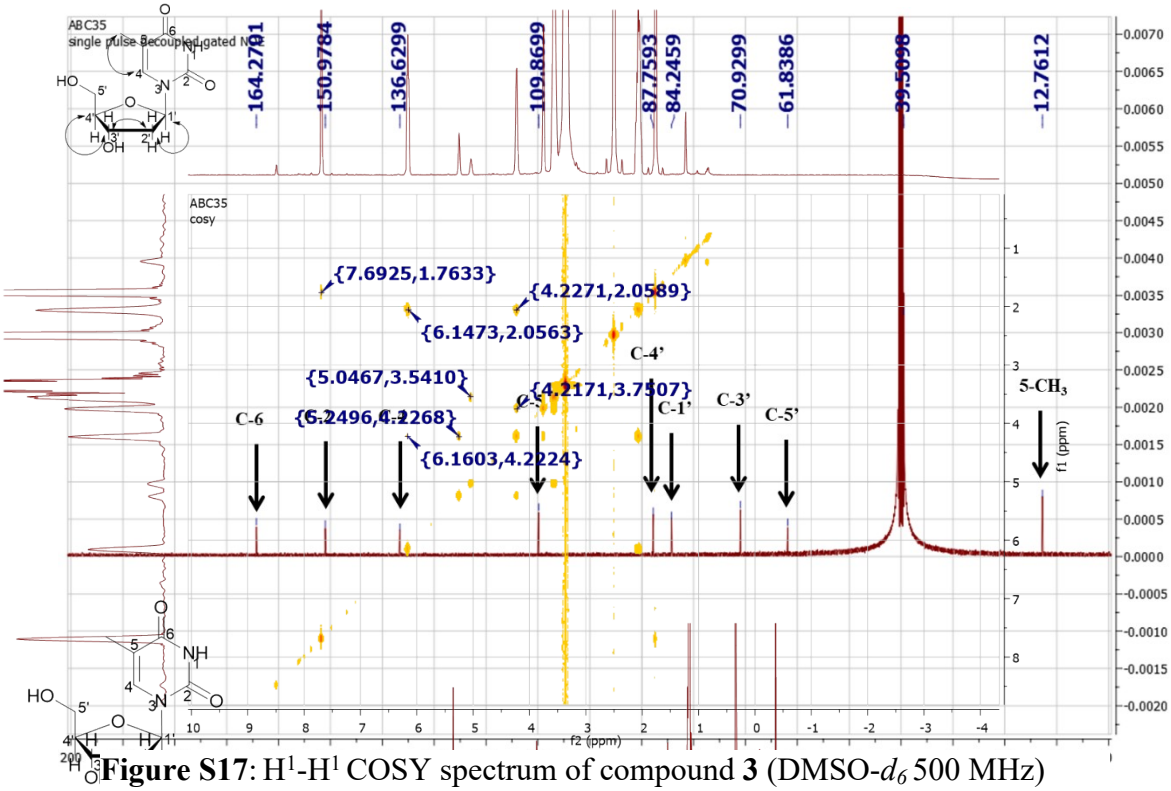

Figure S17: H^{1}-H^{1} COSY spectrum of compound **3** (DMSO-d_6 500 MHz)

Figure S16: ^{13}C- NMR spectrum of compound **3** (DMSO-d_6, 125 MHz)

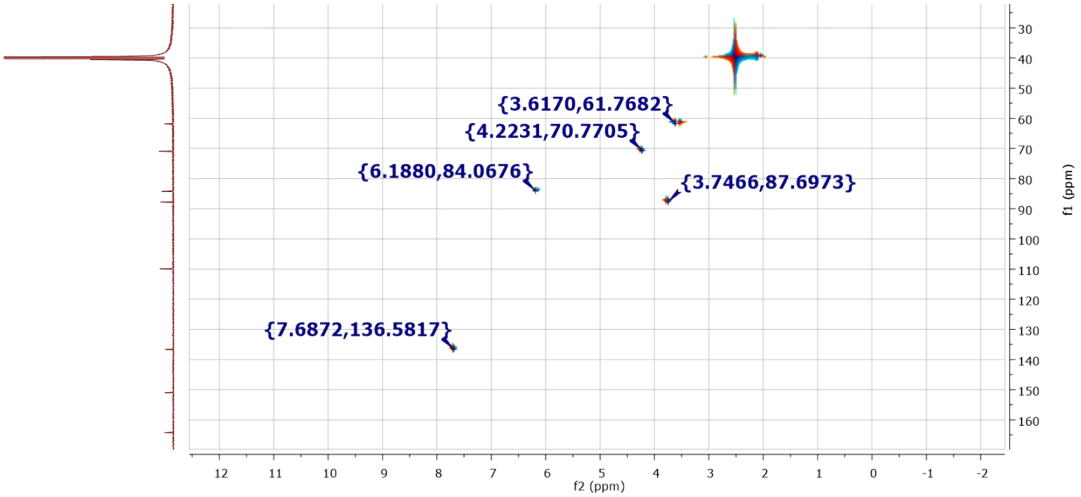

Figure S18: HSQC spectrum of compound **3** (DMSO-d_6, 500 MHz)

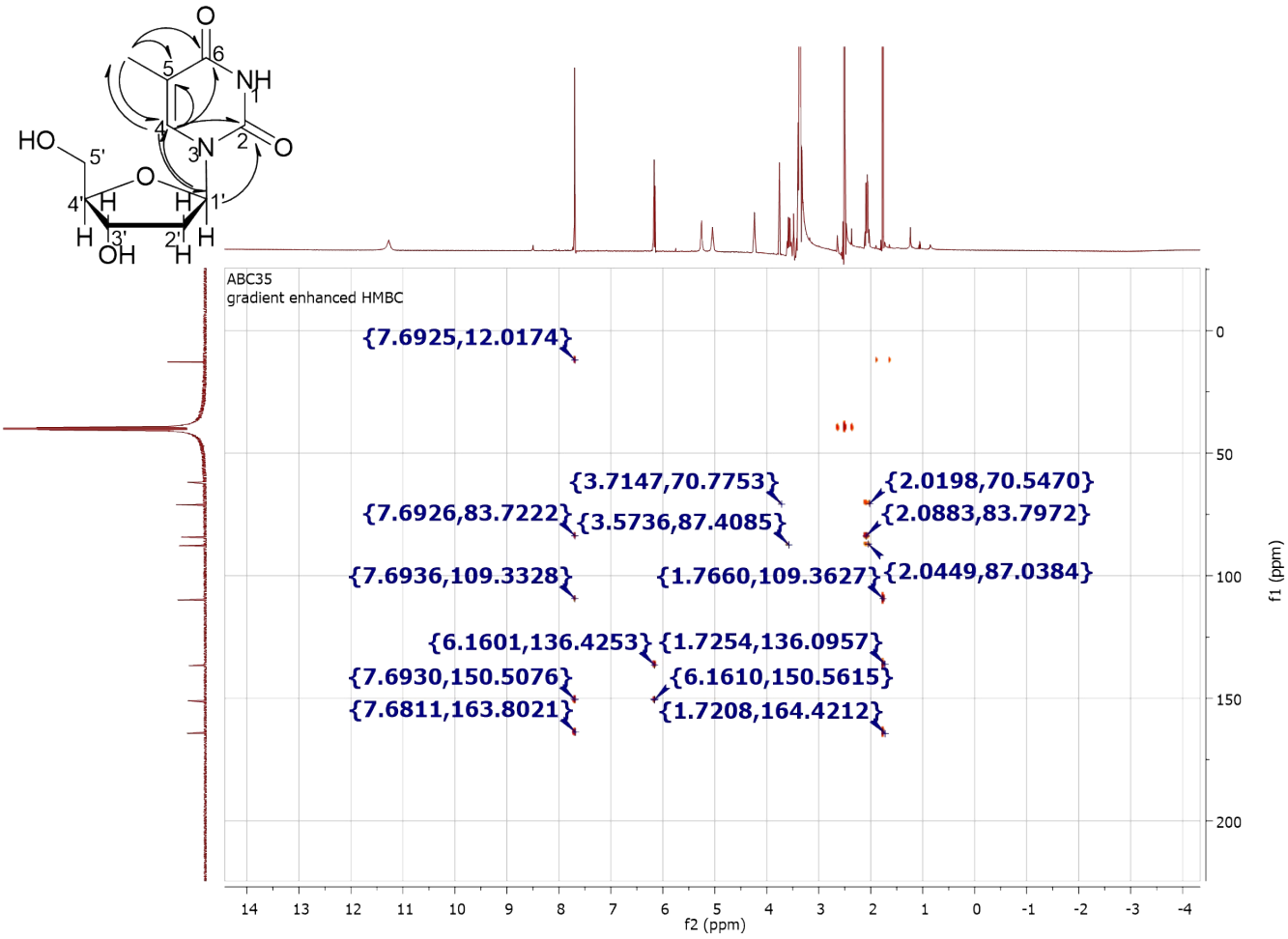

Figure S19: HMBC spectrum of compound **3** (DMSO-d_6, 500 MHz)

NMR spectroscopic analysis of compound (4):

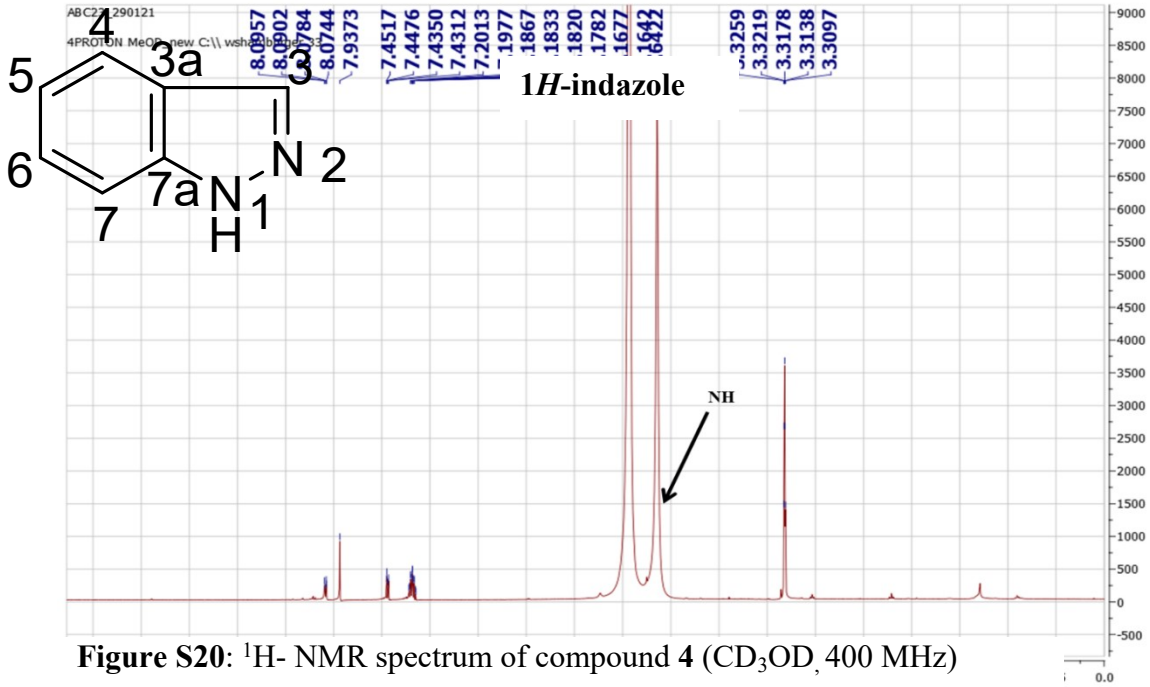

Figure S20: ^{1}H- NMR spectrum of compound **4** (CD_3OD, 400 MHz)

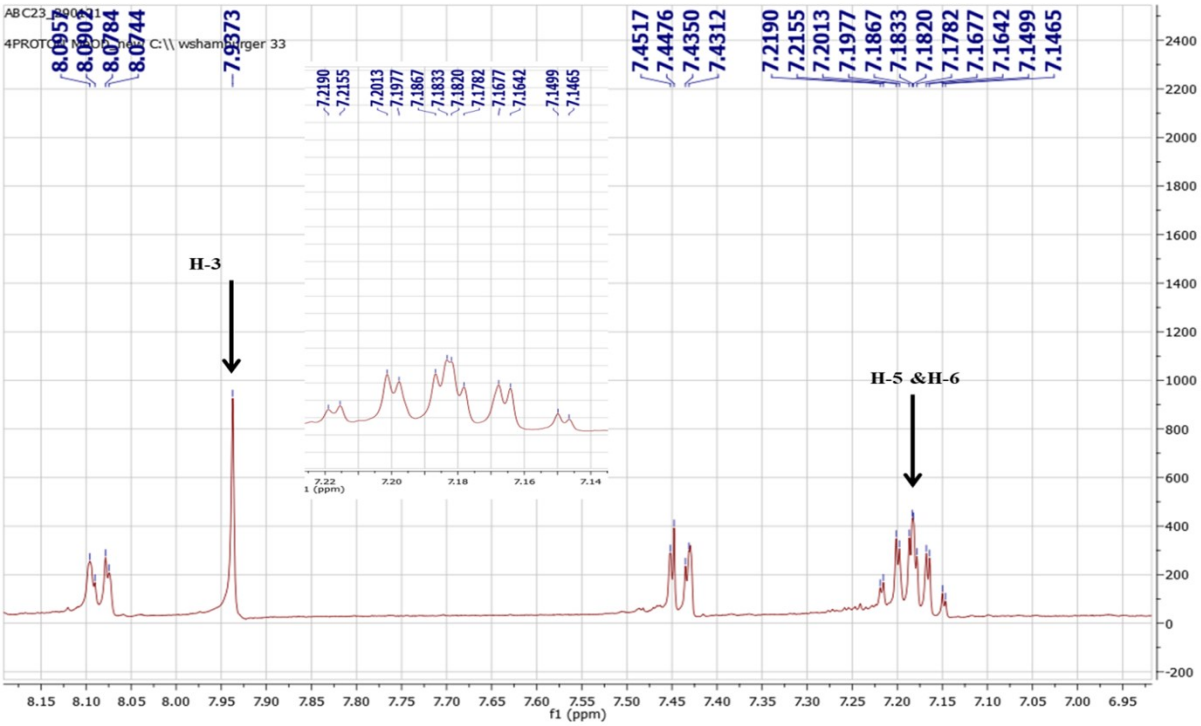

Figure S21: Expanded ^{1}H- NMR spectrum of compound **4** (CD_3OD, 400 MHz)

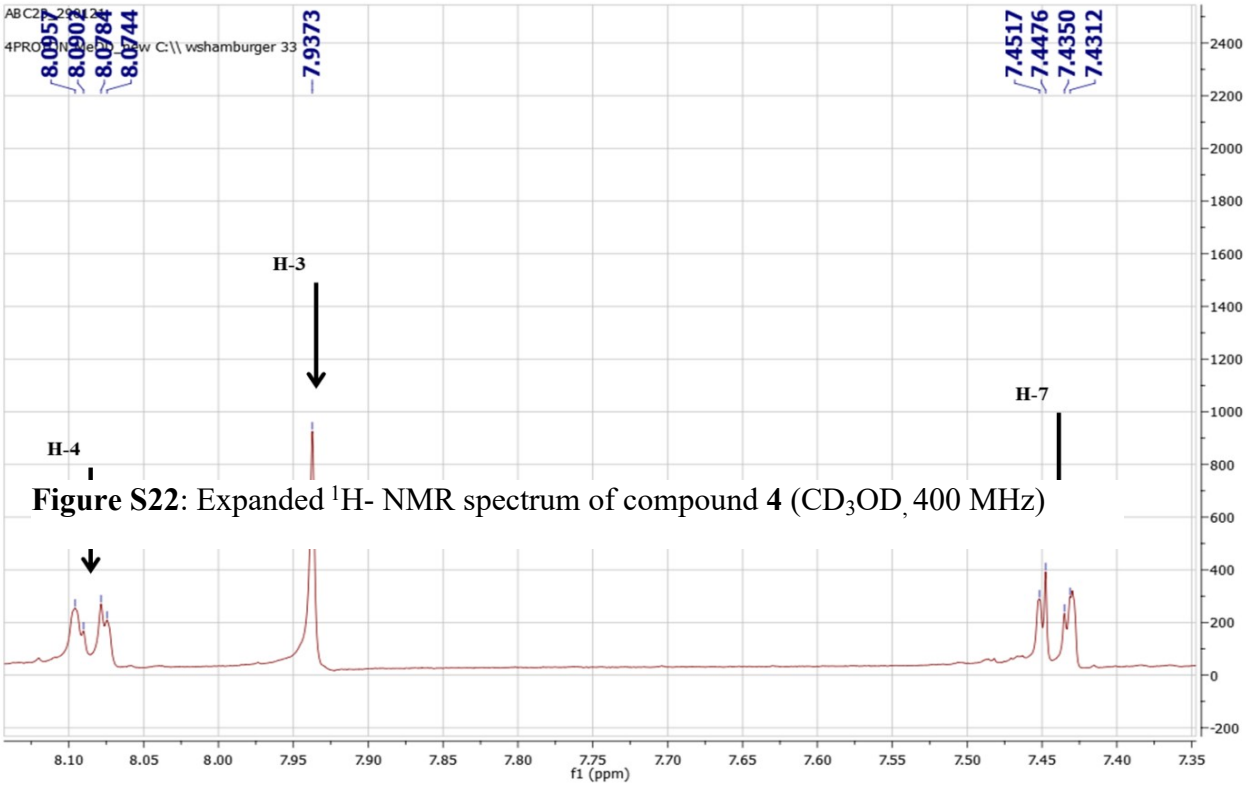

Figure S22: Expanded ^{1}H- NMR spectrum of compound **4** (CD_3OD, 400 MHz)

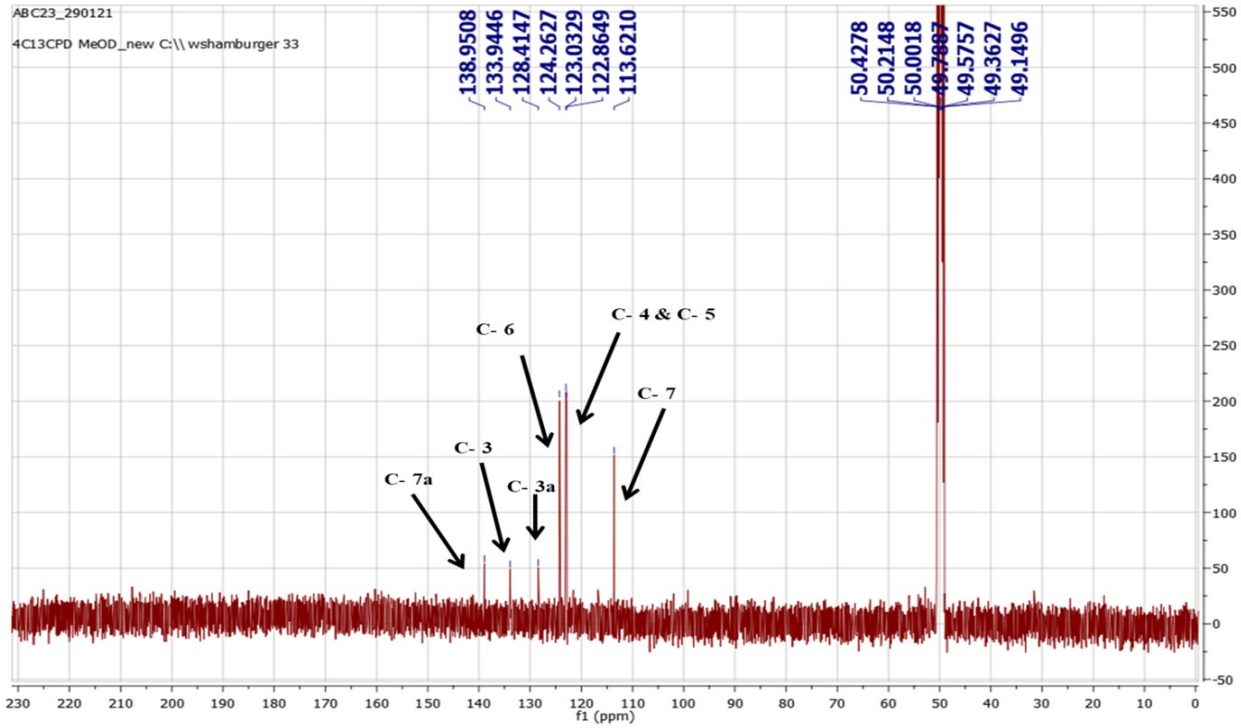

Figure S23: ^{13}C- NMR spectrum of compound **4** (CD_3OD, 100 MHz)

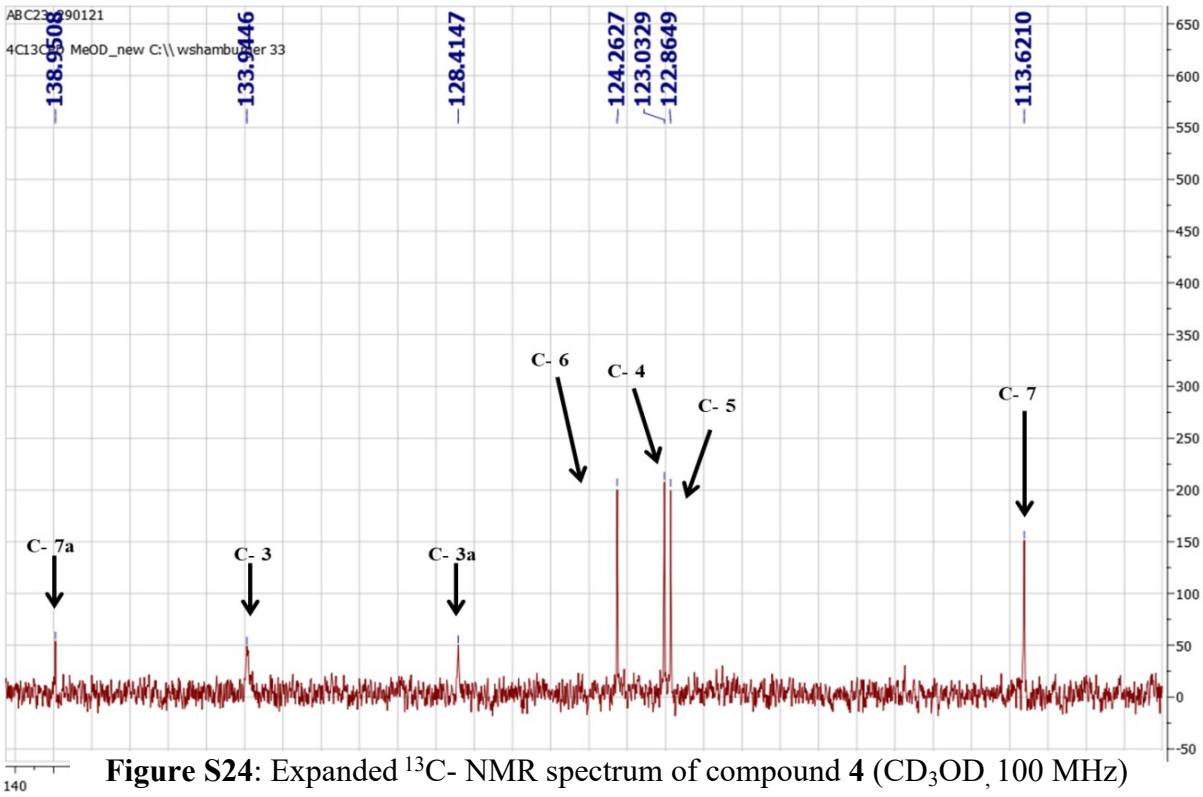

Figure S24: Expanded ^{13}C- NMR spectrum of compound **4** (CD_3OD, 100 MHz)

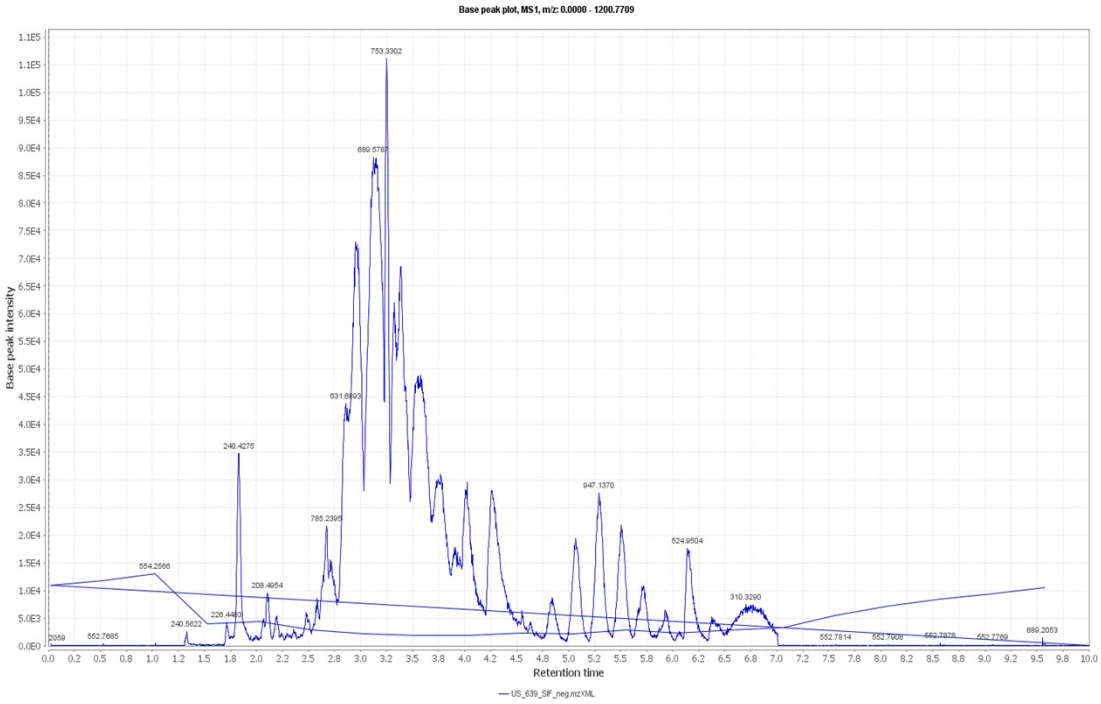

Figure S25: Total ion chromatogram of the ethyl acetate fraction of *Spongia irregularis*.

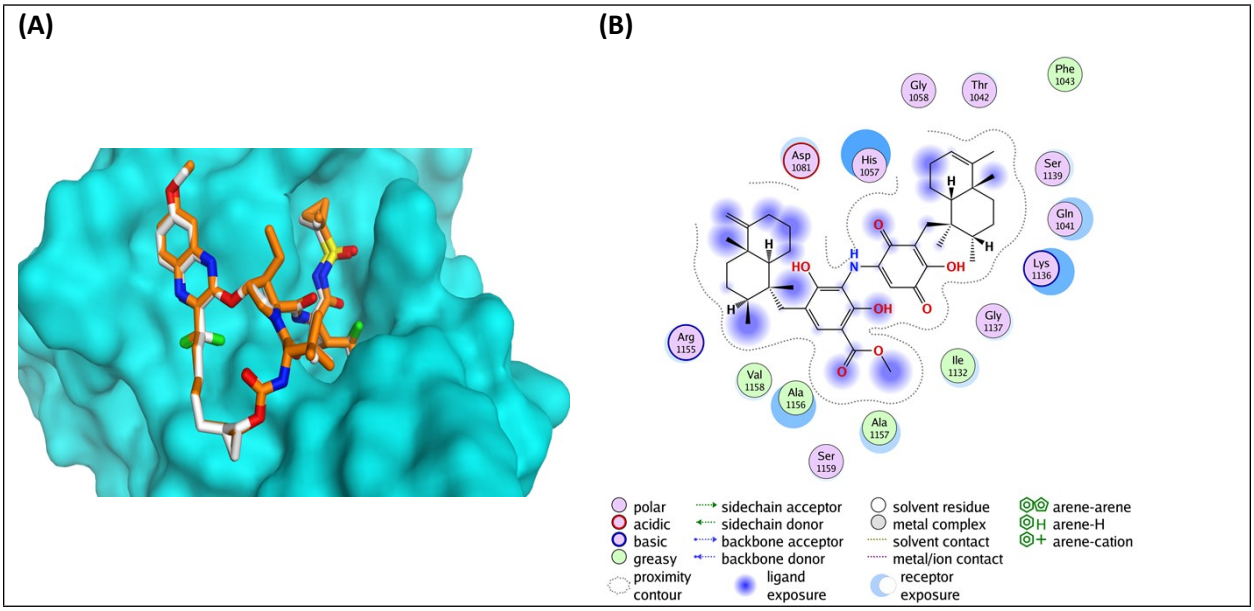

Figure S26:**(A)** Comparison of modelled binding mode of the co-crystallized ligand (white stick model) and its superposed docking conformation (orange stick model) within the HCV NS3 protease active site (PDB code 6NZT) as predicted by MOE 2019.01. **(B)** 2D depiction of compound **13** binding interactions with the critical amino acid residue within the HCV NS3 protease active site (PDB code 6NZT) as predicted by MOE 2019.01.

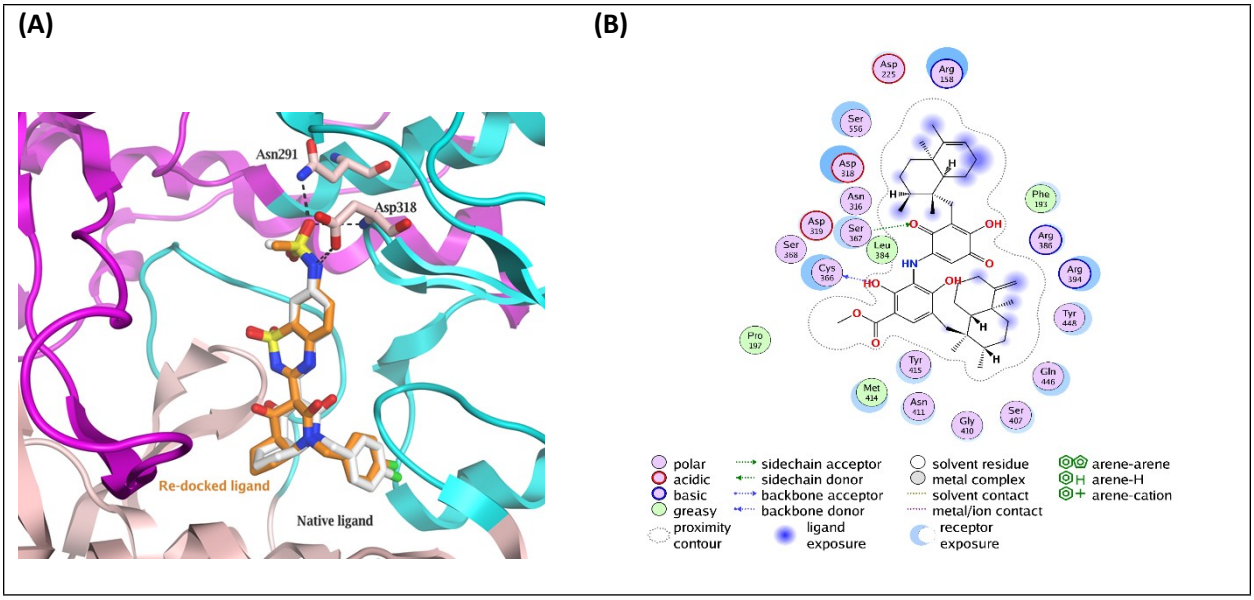

Figure S27:(A) Comparison of modelled binding mode of the co-crystallized ligand (white stick model) and its superposed re-docked conformation (orange stick model) within the HCV NS5B polymerase active site (PDB code: 3H2L) as predicted by MOE 2019.01. **(B)** 2D depiction of compound **13** binding interactions with the critical amino acid residue within the HCV NS5B polymerase active site (PDB code: 3H2L) as predicted by MOE 2019.01.

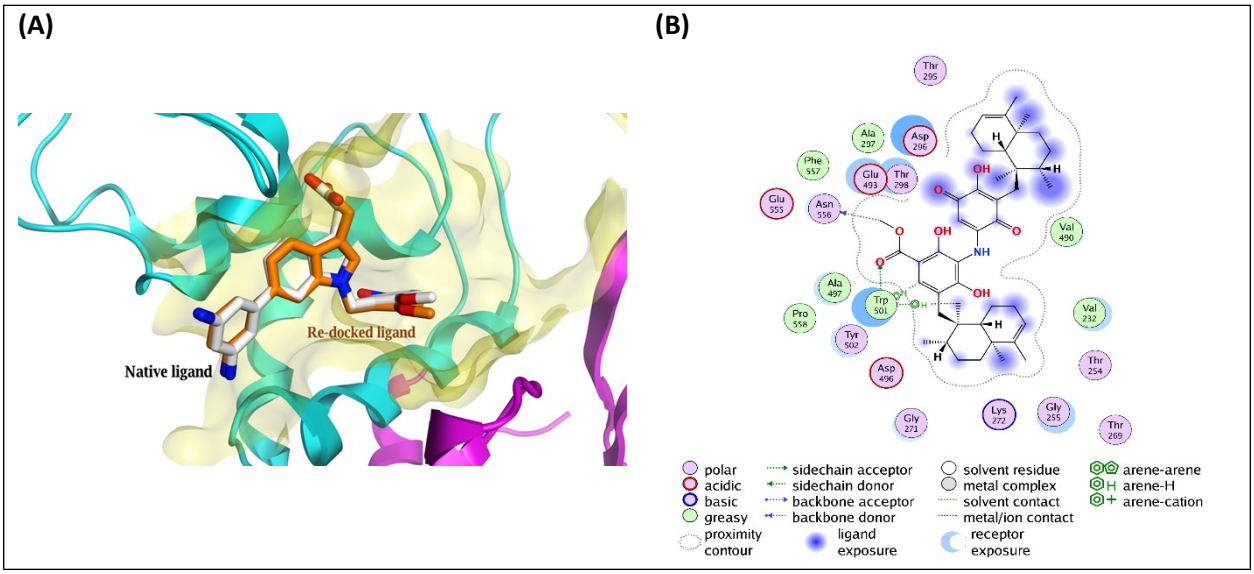

Figure S28:(A) Comparison of modelled binding mode of the native ligand (white stick model) and its superposed re-docked conformation (orange stick model) within the HCV NS3 Helicase active site (PDB code 4OKS) as predicted by MOE 2019.01. **(B)** 2D depiction of compound **14** binding interactions with the critical amino acid residue within the HCV NS3 Helicase active site (PDB code 4OKS) as predicted by MOE 2019.01.

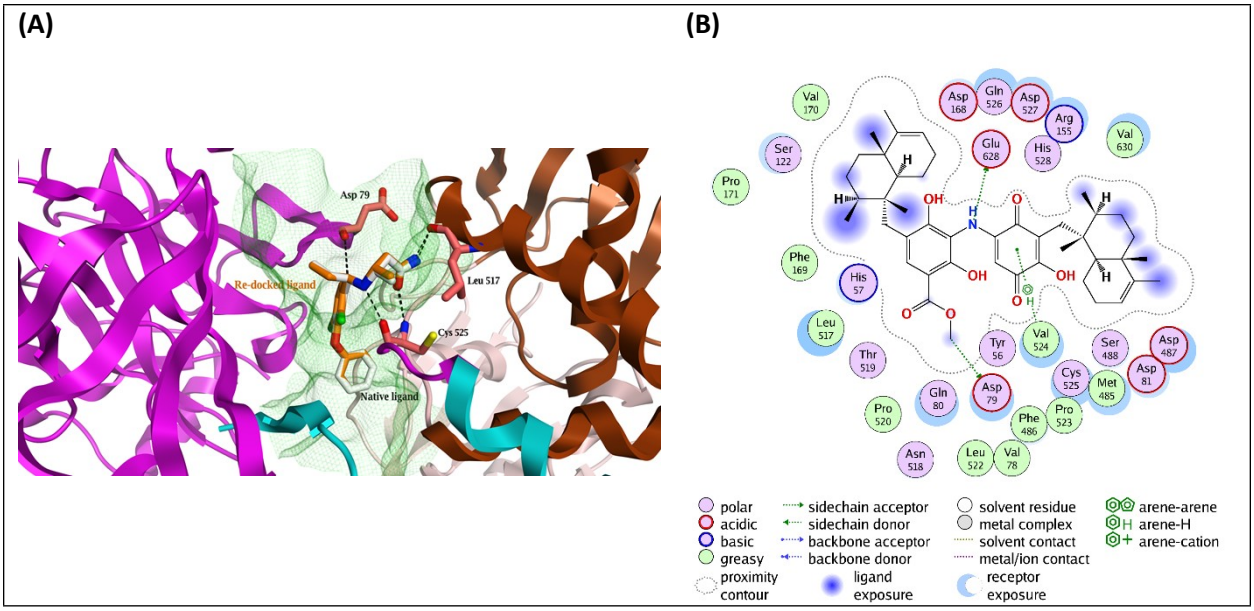

Figure S29:(A) Comparison of modelled binding mode of the native ligand (white stick model) and its superposed re-docked conformation (orange stick model) within the HCV NS3–NS4A protein, located between the protease and helicase domains of the HCV NS3 protein (PDB code: 4B73) as predicted by MOE 2019.01. **(B)** 2D depiction of compound **14** binding interactions with the critical amino acid residue within the HCV NS3–NS4A protein, located between the protease and helicase domains of the HCV NS3 protein (PDB code: 4B73) as predicted by MOE 2019.01.

References:

1. A. R. Carroll, J. Lamb, R. Moni, J. N. A. Hooper and R. J. Quinn, *J. Nat. Prod.*, 2008, **71**, 884-886.
2. L. P. Ponomarenko, A. I. Kalinovsky, S. S. Afiyatullov, M. A. Pushilin, A. V. Gerasimenko, V. B. Krasokhin and V. A. Stonik, *J. Nat. Prod.*, 2007, **70**, 1110-1113.
3. T. Jomori, A. Setiawan, M. Sasaoka and M. Arai, *Nat. Prod. Commun.*, 2019, **14**, 1-7.
4. S. Urban and R. J. Capon, *J. Nat. Prod.*, 1992, **55**, 1638-1642.
5. K. Kobayashi, H. Shimogawa, A. Sakakura, T. Teruya, K. Suenaga and H. Kigoshi, *Chem. Lett.*, 2004, **33**, 1262-1263.
6. K. S. Craig, D. E. Williams, I. Hollander, E. Frommer, R. Mallon, K. Collins, D. Wojciechowicz, A. Tahir, R. Van Soest and R. J. Andersen, *Tetrahedron Lett.*, 2002, **43**, 4801-4804.
7. I. Erdogan Orhan, J. Tanaka, T. Higa and B. Sener, *Nat. Prod. Sci.* , 1999, **5**, 177-180.
8. Y. Takahashi, T. Kubota and J. i. Kobayashi, *Biorg. Med. Chem.*, 2009, **17**, 2185-2188.